The Cryosphere, 19, 5655–5670, 2025 https://doi.org/10.5194/tc-19-5655-2025 © Author(s) 2025. This work is distributed under the Creative Commons Attribution 4.0 License.





Imprints of sea ice, wind patterns, and atmospheric systems on summer water isotope signatures at Hercules Névé, East Antarctica

Songyi $Kim^{1,2}$, Yeongcheol Han^2 , Jiwoong Chung 2 , Seokhyun $Ro^{2,3}$, Jangil $Moon^2$, Soon Do Hur^2 , and Jeonghoon Lee^1

Correspondence: Jeonghoon Lee (jeonghoon.d.lee@gmail.com)

Received: 14 March 2025 - Discussion started: 16 April 2025

Revised: 11 October 2025 – Accepted: 14 October 2025 – Published: 13 November 2025

Abstract. This study investigated the influence of summer climate variability on water isotopes (δ^{18} O, δ^{2} H, and deuterium excess[dexc]) in a Hercules Névé ice core from Antarctica. High-resolution ERA5 reanalysis data for the austral summer (DJF, 1979-2015) were used to assess the relative contributions of temperature, precipitation, wind patterns (v- and u-winds), ocean condition (sea ice concentration [SIC] and sea surface temperature [SST]), and largescale circulation system (Amundsen Sea Low [ASL] and Zonal Wave-3 [ZW3]) to isotopic variability. The results show that higher temperatures and precipitation coincide with isotopically enriched δ^{18} O, confirming their combined role in controlling isotopic enrichment. Wind patterns also contribute meaningfully but in a more complex way: enhanced southerly winds (positive v-wind anomalies) tend to increase δ^{18} O by transporting relatively warm, moisture-rich air from lower latitudes, whereas stronger westerly winds (positive u-wind anomalies) are associated with more depleted isotopic values, likely reflecting colder or more distant moisture sources. Additionally, the dexc exhibits a positive correlation with SIC and negative correlations with SST, providing valuable insights into moisture source processes in the study region during austral summer. Variations in the ASL and ZW3 further modulate heat and moisture transport, reinforcing their role as key atmospheric drivers of isotopic variability. Taken together, these findings suggest that the summer isotope record at Hercules Névé reflects not only local temperature changes but also the broader imprint of ocean-atmosphere interactions, including sea-ice variability

and large-scale circulation patterns. This study highlights the potential of coastal Antarctic ice cores to provide improved constraints on coupled climate processes and to refine paleoclimate reconstructions for the Ross Sea region.

1 Introduction

Stable water isotopes (δ^{18} O and δ^{2} H) have served as crucial proxies for paleoclimatic reconstructions due to their systematic relationship with temperature, making ice cores invaluable archives of past climatic information (Dansgaard, 1964; Jouzel et al., 1997). Recent advancements, such as refined surface temperature reconstructions using advanced modeling approaches (Markle and Steig, 2022) and analyses of isotopic diffusion in snow layers for estimating past temperatures (Holme et al., 2018), highlight the progression from observational studies toward sophisticated modeling. Despite these advancements, accurately interpreting isotopic records from ice cores remains challenging, particularly due to regional variability in the temperature-isotope relationship. In polar regions, and especially across Antarctica, local climatic and atmospheric conditions significantly influence this relationship, creating spatial differences in isotopic signals (Masson-Delmotte et al., 2008; Sime et al., 2009). Therefore, regional investigations are essential to bridge these gaps and improve the interpretation of Antarctic ice-core records.

¹Department of Earth Science Education, Ewha Womans University, Seoul, 03760, Republic of Korea

²Division of Glacier & Earth Science, Korea Polar Research Institute, Incheon, 21990, Republic of Korea

³Department of Ocean Sciences, Inha University, Incheon, 22212, Republic of Korea

Victoria Land in East Antarctica offers unique advantages for understanding climatic processes due to its transitional position between the high interior plateau and the coastal regions. Previous research in this area has utilized ice cores from locations such as Styx Glacier, Talos Dome, Whitehall Glacier and Hercules Névé to study regional climate dynamics (Bertler et al., 2011; Emanuelsson et al., 2023; Masson-Delmotte et al., 2008; Nyamgerel et al., 2024; Sime et al., 2009; Stenni et al., 1999, 2002; Thomas et al., 2017). Each site contributes distinct climatic information: Styx Glacier provides detailed records of local temperature trends (Nyamgerel et al., 2024; Thomas et al., 2017), while Talos Dome captures long-term climatic signals influenced by marine-continental air mass interactions (Frezzotti et al., 2007). Research at Whitehall Glacier has emphasized its role in documenting snow accumulation patterns and their relationship to atmospheric dynamics (Sinclair et al., 2012). These studies have collectively advanced our understanding of isotopic variability and its relationship to atmospheric processes. Among these, Hercules Névé is particularly sensitive to both coastal and interior atmospheric influences due to its proximity to the Ross Sea. The high snow accumulation rates in this region allow for the preservation of detailed isotopic records, which are essential for investigating Antarctic climate variability and its broader global impacts (Masson-Delmotte et al., 2003; Sinclair et al., 2012).

Isotope-enabled general circulation models demonstrate that sea ice extent and concentration modify the isotopic composition of coastal precipitation by altering moisture source regions and transport pathways (Faber et al., 2017; Noone and Simmonds, 2004). Reduced sea ice exposes nearby open ocean areas, enhancing evaporation from local sources and typically leading to enriched δ^{18} O values due to shorter transport distances. Conversely, expanded sea ice displaces evaporation sources farther from the continent, lengthening the distillation pathway and promoting isotopic depletion. However, these relationships vary spatially and seasonally and are influenced by regional circulation, moisture recycling, and synoptic-scale variability (Song et al., 2023). The interaction between sea ice and atmospheric circulation is governed by several major features. The Amundsen Sea Low (ASL) strongly modulates wind direction and moisture transport in the Ross Sea region (Hosking et al., 2013; Raphael et al., 2016), while Zonal Wave 3 (ZW3) influences air-mass distribution and precipitation across coastal Antarctica (Goyal et al., 2022). Regional cyclonic activity also contributes to shaping the isotopic composition of precipitation in coastal Antarctica. This modulation affects regional precipitation isotopes and links sea ice variability with broader atmospheric processes (Emanuelsson et al., 2023; Sinclair et al., 2013).

The Austral summer months of December, January, and February (DJF) are particularly suitable for sea ice research because of the climatic and environmental dynamics observed during this period. For example, Antarctica experi-

ences higher solar radiation levels during DJF, leading to dynamic changes in the extent and structure of sea ice. These katabatic winds flow downslope from the interior year-round and generally intensify in winter; they drive offshore advection/divergence of coastal sea ice and are associated with coastal polynya formation. In winter such polynyas can enhance net sea-ice production through increased heat loss and subsequent freezing (Dale et al., 2020; Turner et al., 2016). These polynyas facilitate the exchange of heat and moisture between the ocean and atmosphere, influencing local and regional climate patterns (Stammerjohn et al., 2015). These conditions enhance both snowfall frequency and isotopic preservation, allowing robust analysis of seasonal variability.

The primary objective of this study was to analyze how stable water isotopes in the Hercules Névé region respond to various climatic drivers during the Austral summer months. While previous studies have predominantly focused on annual or multi-seasonal isotope-climate relationships across Antarctica, the present work isolates the summer signal to examine the processes that shape isotopic variability on shorter timescales. Given the strong seasonality of accumulation and the relative clarity of the isotopic signal during austral summer, this study concentrates on the DJF period. This focus provides the most consistent basis for linking isotopic variations to regional climate processes. Specifically, the relationship between isotopic composition and key climatic variables, such as temperature, precipitation, and u- and vwind components, is evaluated to determine the extent to which isotopic variability reflects both local and synopticscale forcing. By focusing on the DJF period, when coastal meteorology is strongly influenced by sea-ice retreat and enhanced exchange between ocean and atmosphere, this study investigates whether the summer isotope signals preserved at Hercules Névé represent solely local temperature variability or the integrated effects of regional circulation and oceanic conditions. In particular, the analysis addresses (1) the extent to which δ^{18} O variability is modulated by precipitation and circulation in addition to temperature, and (2) whether dexc can serve as a sensitive tracer of sea-ice concentration and sea surface temperature. Through this approach, we aim to advance a process-based understanding of water-isotope variability in coastal Antarctica. High-resolution water isotope analysis with ERA5 reanalysis data, atmospheric circulation indices (ASL and ZW3) and back trajectory modeling. Correlation and principal component analyses were used to evaluate the relationships between isotope variability and climatic drivers, thereby linking synoptic-scale circulation and ocean-atmosphere processes to the isotopic signal preserved at Hercules Névé.

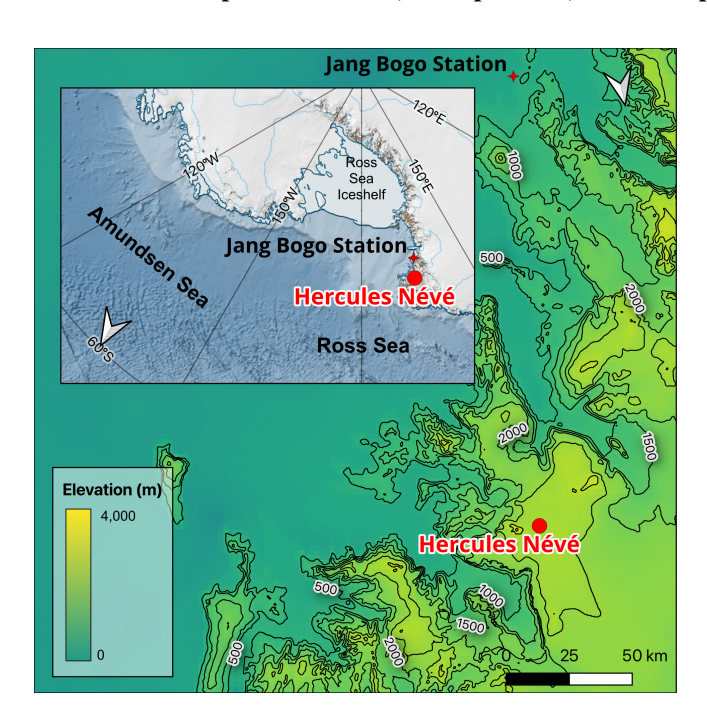


Figure 1. (A) Map of the West and East Antarctica regions showing the Ross Ice Shelf, the Ross Sea, and Hercules Névé. (B) Topographic map of Northern Victoria Land. The red circles indicate the location of the Hercules Névé ice core. The maps were created using Quantarctica 3.2 on QGIS.

2 Materials and methods

2.1 Study Area

The research area is located at Hercules Névé, Victoria Land, Antarctica, at 73°03′ S, 165°25′ E (Fig. 1). Situated at an altitude of 2864 m and approximately 80 km inland from the sea, the climatic conditions of this mountainous area are affected by its position near the northern edge of the Transantarctic Mountains, which strongly influence atmospheric circulation by acting as a barrier to the flow of air masses (Tewari et al., 2021). Because the interaction between the mountains and the prevailing winds generates various microclimates at Hercules Névé, it has become an area of interest for understanding the complex interactions between the local geography and climate (Maggi and Petit, 1998).

Victoria Land has long been used as a research site to study the impact of atmospheric and oceanic variability on snow accumulation and ice core records (Maggi and Petit, 1998; Nardin et al., 2020; Nyamgerel et al., 2024; Yan et al., 2021; Yang et al., 2018). This region is characterized by austral summer-dominant precipitation patterns influenced by easterly winds that bring moist air from the ocean onto the continent (Scarchilli et al., 2011). Katabatic winds descending from the East Antarctic Plateau are typically cold and extremely dry. Their dryness enhances sublimation from the snow surface, which can lead to isotopic modification

of near-surface layers (Nyamgerel et al., 2024; Vihma et al., 2011). However, their impact on local temperature and the surface energy balance is not always unidirectional and may vary depending on synoptic conditions (Davrinche et al., 2024). Broader climatic drivers such as the Southern Annular Mode and sea ice variability also impact regional weather patterns and precipitation (Yang et al., 2018). Hercules Névé is thus a useful site for the analysis of how regional climate variability influences snow deposition and ice core records, which can be used to reconstruct past climate conditions. Furthermore, previous studies have reported a high snowfall rate in the surrounding area (Maggi and Petit, 1998; Nyamgerel et al., 2020; Stenni et al., 1999, 2000), making this region particularly suitable for ice core seasonal analysis.

2.2 Data Acquisition

2.2.1 Sampling and Water Isotope Data

To acquire water isotope data from Hercules Névé in northern Victoria Land, an ice core was drilled between 11 and 15 December 2015, according to the method described by Han et al. (2015). The ice core was extracted to a depth of approximately 80 m, was immediately segmented, sealed in plastic bags, logged, and packaged in insulated containers to prevent temperature fluctuations during transport to a laboratory at the Korea Polar Research Institute (KOPRI). After drilling was completed in December 2015, the Hercules Névé ice core was transported to the KOPRI, where it was stored frozen until cutting. In the second half of 2017, the core was cut into 5 cm segments in a clean laboratory environment to ensure seasonal-scale resolution.

In the laboratory, the ice core was carefully segmented into 5 cm sections based on analytical needs to assess seasonal variability, yielding approximately 2000 segments. This segment size was selected to ensure data representativeness and ease of handling by providing a balance between resolution and sample manageability. Each segment was processed in a clean environment to prevent contamination. The ice was melted at room temperature in sealed containers to avoid isotopic fractionation via physical processes such as evaporation and sublimation. The meltwater was filtered through 0.45 µm syringe filters to remove particulates and transferred into 2 mL high-density polyethylene (HDPE) vials with airtight caps to prevent isotopic exchange with ambient air.

All samples were stored at temperatures below 4 °C and were analyzed within 12 months of preparation to ensure isotopic stability. The liquid samples were analyzed using a Picarro L2130-i water isotope analyzer, which employs cavity ring-down spectroscopy (CRDS) for high-precision measurements. The analyzed water isotope results were expressed using delta notation, as shown in Eq. (1):

$$\delta(\%_0) = (R_{\text{sample}}/R_{\text{standard}} - 1) \times 1000 \tag{1}$$

The secondary parameter deuterium excess (dexc), defined according to Dansgaard, (1964), was also determined as shown in Eq. (2):

$$dexc = \delta^2 H - 8 \times \delta^{18} O \tag{2}$$

Measurement precision was $\pm 0.07\%$ for δ^{18} O and $\pm 0.1\%$ for δ^2 H, based on long-term repeated measurements of laboratory standards conducted over multiple years. The measurements were calibrated using the international standards VSMOW, Greenland Ice Sheet Precipitation (GISP), and Standard Light Antarctic Precipitation (SLAP), as well as the laboratory standard RS $(-34.69 \pm 0.07\% \text{ for } \delta^{18}\text{O},$ $-272.4 \pm 0.6\%$ for δ^2 H). The measurements followed the internal analytical protocol used at KOPRI, as described in (Kim et al., 2022). Each sample was injected 12-15 times, and the average of the final 5 measurements was used to ensure thermal and instrumental stability. International reference waters (VSMOW, SLAP, GISP) were measured every \sim 100 samples for calibration, and laboratory reference waters were measured after every 10 unknowns to monitor analytical consistency. This procedure ensured high precision and long-term stability of the isotope measurements.

2.2.2 Utilization of ERA5 Data and ZW3 Data

In this study, we utilized ERA5 reanalysis data provided by the European Centre for Medium-Range Weather Forecasts (ECMWF, covered on a 31 km grid) (Hersbach et al., 2020). ERA5 variables used in this analysis include 2 m air temperature $(T_{2 \text{ m}})$, 10 m u- and v-wind components, mean sea level pressure (MSLP), sea surface temperature (SST), and sea ice concentration (SIC). ERA5 has been widely validated for use in Antarctica due to its high temporal and spatial resolution and strong correlation with observational data (Tetzner et al., 2019). To assess the accuracy of reanalysis data in representing local atmospheric conditions, an automatic weather station (AWS) was installed at the Hercules Névé site during the drilling campaign, recording air temperature, wind speed, and wind direction over one year. The AWS dataset was compared with ERA5 outputs for the same period, focusing on temperature and wind variables (Figs. S1 and S2 in the Supplement). ERA5 reproduces general patterns in temperature and wind direction well. However, it tends to overestimate summer (DJF) temperatures relative to AWS, as shown by the DJF AWS-ERA5 comparison using a York regression analysis (Fig. S1C; $R^2 = 0.57$). Despite this warm bias, ERA5 provides consistent temporal coverage from 1979 to 2015, making it suitable for evaluating interannual climate-isotope relationships in this remote region. Wind direction and speed distributions also show notable differences between AWS and ERA5 (Fig. S2). ERA5 indicates a dominant southerly to southeasterly wind regime during DJF, in line with broader synoptic circulation over the Ross Sea. In contrast, AWS data show more variable wind directions and stronger speeds, likely reflecting local topographic effects and boundary-layer dynamics. For the main analysis, ERA5 fields were extracted at a monthly resolution for the period 1979–2015. To match the temporal resolution of the ice core isotope data, we calculated austral summer means from the monthly data, thereby obtaining one representative seasonal value per year. These DJF-avearged datasets were used for spatial correlation and circulation analyses linking isotopic variability with temperature, precipitation, wind, sea ice, and oceanic conditions.

In addition, the monthly ZW3 index from Goyal et al. (2022), which is derived from ERA5 sea level pressure fields was used to represent large-sale wave activity in the Southern Hemisphere. ZW3 is characterized by three quasi-stationary ridges and troughs in the mid-latitudes of the Southern Hemisphere that influence atmospheric circulation and sea ice distribution around Antarctica (Goyal et al., 2022; Raphael, 2007). The inclusion of the new ZW3 data allows for a more detailed assessment of its impact on the climatic conditions at Hercules Névé via isotopic signatures.

2.3 Data Processing

2.3.1 Age Dating

Manual layer counting is widely used for the age dating of ice cores, with the identification of annual layers relying on variation in proxies such as stable water isotopes (δ^{18} O, δ^{2} H, and dexc), ion concentrations, dust deposition, and electrical conductivity method (ECM) (Johnsen et al., 2001; Masson-Delmotte et al., 2003; Sigl et al., 2016; Sinclair et al., 2012). Previous studies have demonstrated that, in regions with abundant snowfall, particularly along coastal areas, water isotope signals are well-preserved and exhibit clear seasonal cycles, allowing for the precise manual counting of annual layers. Seasonal variation in δ^{18} O, δ^{2} H, and dexc from the Hercules Névé ice core, characterized by higher $\delta^{18}O$ and δ^2 H values during warmer months and lower values during colder periods, were thus used to establish annual layers for age dating (Fig. 2B-D). This method provides a highresolution age model based on stable water isotope variation, which can be linked to specific years and climatic events. Annual layers were identified from the seasonal oscillation in the isotope profiles (δ^{18} O, δ^{2} H, and dexc) by visual inspection of peak-trough cycles. Phase consistency among δ^{18} O, δ^2 H, and dxc was required to assign the seasonal transitions.

Radioactive isotopes resulting from atmospheric nuclear testing, such as plutonium-239 (²³⁹Pu) and tritium, can be utilized to validate the accuracy of the manual layer counting method (Hwang et al., 2019; Stenni et al., 1999). In this study, ²³⁹Pu concentrations were measured at various depths within the Hercules Névé ice core, and ²³⁹Pu peaks corresponding to known periods of atmospheric nuclear testing in the late 1950s and early 1960s were employed as absolute time markers (Fig. 2A). By matching these peaks with the historical records for nuclear testing, we confirmed the

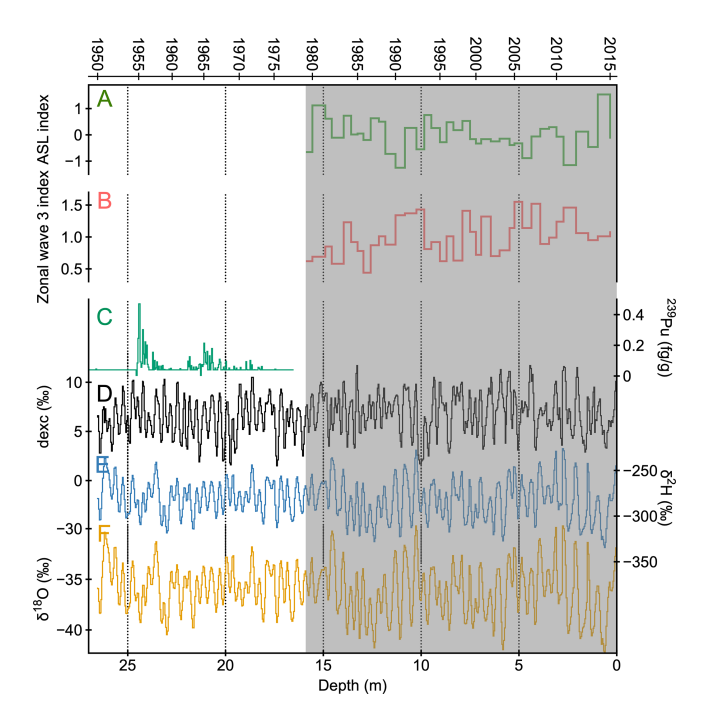


Figure 2. Depth profiles of climate indices and isotopic parameters from the surface to a depth of 26 m from the Hercules Névé ice core. Panel (**A**) represents the Amundsen Sea Low (ASL) index derived from principal component analysis (PCA) based on longitude, latitude, and strength of the ASL defined in Hosking et al. (2013), specifically displaying PC3, which showed significant correlation with isotopic data. Panel (**B**) shows the Zonal Wave 3 (ZW3) index obtained from Goyal et al. (2022). Panel (**C**) depicts the 239Pu concentration profile for the period 1950–1975. Panels (**D**)–(**F**) illustrate water isotope measurements (dexc, δ^2 H, and δ^{18} O, respectively) spanning from 1950 to 2016. Data utilized for detailed analysis in this study (1979–2015) are indicated by the shaded grey region.

age of specific layers and validated the annual layer counting method. The uncertainty for the age dating of the ice core was assumed to be less than a year.

In this study, we successfully determined the ice core chronology back to the 1950s, reaching a depth of approximately 25 m. For isotopic and climate analysis, we used the top 16 m of the core, which represents roughly 40 years of accumulation (highlighted in grey in Fig. 2). Clear seasonal cycles in $\delta^{18}O$ and dexc enabled manual annual layer counting to construct a high-resolution age-depth model. The estimated mean annual snowfall over this period was $204.5 \,\mathrm{kg}\,\mathrm{m}^{-2}\,\mathrm{yr}^{-1}$ or ± 54.5 . Within each annually dated layer, each sample point (typically 5–15 yr⁻¹) was assigned a fractional year value based on its relative depth position. To assign calendar months, the $\delta^{18}O$ maximum within each year was used as an anchor point and fixed to January, representing the midpoint of the austral summer. All other sample positions were then linearly interpolated across the year. Linear interpolation between successive isotope extrema was applied to obtain an approximately monthly-resolved series within each annual layer. The DJF δ^{18} O series derived from this interpolation was then aligned, year by year, with DJFaveraged ERA5 fields (1979-2015) to ensure temporal consistency for correlation analyses. While this approach assumes that $\delta^{18}O$ peaks reflect summer accumulation, the use of DJF averages, centered around the $\delta^{18}O$ maximum and spanning three months, minimizes sensitivity to shortterm variability in peak timing. This interpolation allowed for monthly-resolved isotope estimates, including months not directly sampled. From this monthly-interpolated series, DJF values were extracted and averaged to produce an annual DJF $\delta^{18}O$ time series from 1979 to 2015. This time series was subsequently used in correlation analyses with ERA5derived temperature, precipitation, and wind data to interpret climatic influences on isotopic variability.

2.3.2 Statistical Analysis

We applied several statistical methods to evaluate the relationship between water isotopes and various climatic drivers in the Hercules Névé region. All climate variables were obtained from the ERA5 reanalysis dataset (Hersbach et al., 2020) for the period 1979–2015, including 2 m air temperature (T_{2m}) , total precipitation (tp), 10 m u- and v-wind components, and sea ice concentration (SIC). ERA5 data were extracted over the sector 70-77° S, 160-170° E, encompassing the northern Victoria Land region. Monthly fields were averaged to derive DJF means for each year, matching the temporal resolution of the isotope record. Spatial correlation analysis was performed between the δ^{18} O time series and gridded ERA5 climate fields to identify dominant spatial patterns. Pearson correlation coefficients were computed on a seasonal (DJF) basis to assess spatially coherent relationships (e.g., Sime et al., 2009; Thomas et al., 2017).

To examine large-scale circulation drivers, we used a monthly Zonal Wave 3 (ZW3) index developed by Goyal et al. (2022) and the Amundsen Sea Low (ASL) diagmostics provided by the British Antarctic Survey (Hosking et al., 2013). The ASL parameters (central pressure, latitude, and longitude) were standardized and subjected to Principal Component Analysis (PCA) using a correlation matrix to identify coupled spatial-intensity modes of ASL variability (Coggins and McDonald, 2015). The resulting PCs were correlated with $\delta^{18}O$ to determine which modes had the strongest association with isotopic variability. To investigate broader circulation patterns, we performed Empirical Orthogonal Function (EOF) analysis of 500 hPa geopotential height fields for DJF, following standard methods (e.g., Raphael et al., 2016; Clem et al., 2017). The corresponding principal components were used to interpret SAM- and ZW3like structures and their association with δ^{18} O variability.

Lastly, to assess atmospheric moisture pathways, we used the HYSPLIT model (Stein et al., 2015) to compute 7 d backward trajectories arriving at Hercules Névé (73°03′ S, 165°25′ E). Trajectories were initialized four times (00:00, 06:00, 12:00, 18:00 UTC) for the DJF period (1979–2015) using GDAS 1° × 1° meteorological data. fields for the DJF months from 2006 to 2015. Cluster analysis was conducted on the ensemble of trajectories for this 10-year period using the Euclidean distance criterion, and three clusters were selected to represent the dominant moisture-transport regimes. Composite trajectories were then generated separately for summers with a strong ASL (2008, 2009, 2015 and 2016) and weak ASL (2006, 2010, 2013 and 2014), based on the ASL strength index from Hosking et al. (2013). These composites illustrate the contrasting moisture-source regions and transport pathways associated with variations in ASL intensity.

To assess the signal-to-noise ratio and test whether the δ^{18} O record contains a preserved seasonal signal, we performed a Lomb–Scargle periodogram analysis. As shown in Fig. S3, the spectrum exhibits a statistically significant peak at $1\,\mathrm{yr}^{-1}$ (p < 0.05), indicating that the time series retains a robust seasonal (annual) cycle. This result supports the use of DJF-averaged isotope values for climate correlation analysis and justifies the seasonal aggregation approach used throughout this study.

To check whether post-depositional processes bias our summer signal, we evaluated the DJF δ^{18} O-dexc relationship following Casado et al. (2021). In this framework, negative relationships imply substantial modification, whereas positive relationships suggest minimal alteration. For Hercules Névé, the δ^{18} O-dexc relationship is positive during DJF (r=0.51), consistent with limited post-depositional modification. Although a positive slope generally indicates preservation of the primary isotopic signal (Casado et al., 2021), recent study from surface snow at EastGRIP show that weak positive slopes may still arise under conditions of minor post-depositional alteration (Town et al., 2024). Therefore, while our data suggest that the summer isotopic signal has been largely preserved, small-scale re-equilibration effects cannot be entirely excluded.

3 Results

3.1 Water Isotope Records in the Ice Core from Hercules Névé

Figure 2 presents the water isotope data from Hercules Névé for the period 1979–2015. The δ^{18} O values ranged from -42.29% to -29.67%, with a standard deviation of 1.69%, while those for δ^2 H ranged from -334.5% to -226.1%, with a standard deviation of 11.75%. These values are comparable to other near-coastal Antarctic sites in Victoria Land, such as Styx–M, Whitehall Glacier, and Talos Dome, which represent a range of altitudes and moisture conditions (Table S1 in the Supplement).

Using the annual mean $\delta^{18}O$ and $\delta^{2}H$ in Hercules Névé core, we derived a local meteoric water line (LMWL) with a slope of 8 and an intercept of 8.2 ($R^{2}=0.99$). While there slope and intercept are higher than those of the Antarctica meteoric water line (AMWL, slope = 7.75 and intercept = -4.93 Masson-Delmotte et al., 2008), yet similar to the global meteoric water line (GMWL, slope = 8 and intercept = 10; Craig, 1961). The similarity suggests that, owing to its coastal proximity, the Hercules Névé region, experiences moisture conditions more characteristic of oceanic environments, resulting in a steeper $\delta^{18}O-\delta^{2}H$ relationship (Fernandoy et al., 2010; Goursaud et al., 2018; Nyamgerel et al., 2024).

Seasonally, the $\delta^{18}O-\delta^2H$ relationship in the Hercules Névé core range from 8 to 8.3 and 7.8 to 18 (Fig. S4). During the austral summer, the slope (8.0) and the intercept (7.8)closely match the annual LMWL, indicating that the summer precipitation is more likely to reflect the temperatureisotope relationship with minimal post-depositional alteration. ERA5 reanalysis data from 1979-2015 show that precipitation minus evaporation during DJF accounts for approximately 23 %–40 % (mean 35 %, standard deviation 4 %) of the annual total. While DJF does not dominate the annual accumulation in terms of volume, it occurs under conditions of relatively frequent snowfall, warmer atmospheric temperatures, and higher moisture flux from open ocean areas due to reduced sea ice extent. Such conditions may enhance the direct imprint of summer climatic signals into the isotopic composition of snow, making the DJF season particularly valuable for interpreting isotope-climate relationships in coastal Antarctica.

To confirm that this seasonal signal is preserved without significant isotopic smoothing, we empirically estimated the diffusion length from the $\delta^{18}O$ time series using a spectral fitting approach (Münch et al., 2016). The resulting diffusion length of approximately 6 cm, comparable to the 5 cm sampling interval, indicates that seasonal variability is well resolved at this resolution and that the isotopic cycles retain their original amplitude.

3.2 Impact of Summer Climate Patterns on Water Isotope in the Antarctic Hercules Névé

Using ERA5 climate reanalysis data for 1979–2015, we examined how temperature, precipitation, and wind components (v- and u-winds) relate to δ^{18} O variability during thre austral summer (DJF) at Hercules Névé site (Fig. 3). When using annual mean temperature, δ^{18} O shows a weak correlation (r=0.13 likely due to the superposition of several process that obscure a direct isotopic–thermal relationship: varying moisture sources (Masson-Delmotte et al., 2008; Noone and Simmonds, 2004), strong synoptic variability associated with the Ross Sea region (Schlosser et al., 2016), seasonal difference in precipitation frequency (Casado et al., 2018), and post-depositional modifications of the surface

snow (Casado et al., 2021; Mahalinganathan et al., 2022). Such effect dilute the annual isotope–temperature signal, underscoring the limitations of paleoclimate reconstructions based solely on annual mean annual signatures (Laepple et al., 2025).

By contrast, the austral summer correlation between $\delta^{18}O$ and temperature is more pronounced $(r=0.32,\ p<0.05;\ slope of <math>0.59\,\%e^{\circ}C^{-1}$). Although slightly lower than the Styx site $(0.66\,\%e^{\circ}C^{-1};\ Nyamgerel$ et al., 2024), this summer slope is comparable to other East Antarctic locations such as Whitehall Glacier $(0.62\,\%e^{\circ}C^{-1};\ Sinclair$ et al., 2012), Taylor Dome $(0.50\,\%e^{\circ}C^{-1};\ Steig$ et al., 2000) and Talos Dome $(0.60\,\%e^{\circ}C^{-1};\ Stenni$ et al., 2002) (Fig. S5). This consistency demonstrates that isotope–temperature scaling at Hercules Névé is regionally coherent despite differences in topography and moisture-transport pathways. It also highlights the necessity of seasonal discrimination, while annual values are confounded, summer months preserve the most direct temperature signature (Sinclair et al., 2013).

Several factors may account for this stronger summer correlation: (1) reduced impact of post-depositional process under high accumulation rates, despite enhanced metamorphism under warmer conditions (Town et al., 2008; Waddington et al., 2002), (2) simplified moisture transport pathways during summer circulation (Helsen et al., 2005), and (3) a higher frequency of precipitation events, leading to more direct incorporation of local climatic signals into the ice (Steen-Larsen et al., 2011). Together, these mechanisms indicate that δ^{18} O in summer snowfall is more directly coupled to surface air temperature. These mechanisms imply that δ^{18} O in summer snowfall is a more directly associated by surface air temperature. Precipitation shows positive correlation with δ^{18} O during summer (r = 0.6; Fig. 3B), exceeding its annual mean correlation (r = 0.3, not shown). This pattern suggests that precipitation in coastal Antarctica is often isotopically enriched during periods of heavy snowfall, reflecting moisture sourced from the nearby ocean (Servettaz et al., 2020 and Jackson et al., 2023).

For wind components, the austral summer v-wind (southerly) and u-wind (westerly) are generally negative values, indicating prevailing southerly and westerly winds flows. A positive correlation was observed between $\delta^{18}O$ and v-wind, suggesting that stronger southerly winds are associated with isotopically enriched snowfall (Fig. 3C). Although this relationship may appear counterintuitive, it likely reflects inland advection of mixed continental-oceanic air masses with higher isotopic (Clem et al., 2017; Noone and Simmonds, 2004). Conversely, δ^{18} O is negatively correlated with the u-wind (Fig. 3D), indicating that intensified westerlies transport colder, isotopically depleted air from marine sectors west of the Ross Embayment (Markle et al., 2012). There findings emphasize that temperature, precipitation, and wind directions collectively modulated isotopic variability in the Hercules Névé region.

During DJF, the Hercules Névé ice core record shows a clear co-variation between dexc and local ocean-ice conditions. When SIC is higher, dexc is generally higher, and when SST is higher, dexc is generally lower (Fig. 4A, B). Taken together with the δ^{18} O-climate associations described above, this DJF dexc pattern suggests that summertime isotopic variability at Hercules Névé, located near the Ross Sea, is most closely related to local ocean-ice conditions and polynya-influenced moisture sources. This highlights that not only temperature and precipitation but also moisture source variability has a discernible influence on the isotopic signal, reinforcing the value of summer snowfall as a recorder of regional climate (Noone and Simmonds, 2002; Risi et al., 2010; Uemura et al., 2008).

In summary, the combination of temperature, precipitation, and wind patterns during austral summer exerts a marked influence on δ^{18} O. These results provide a process-based framework for interpreting how coastal Antarctic ice cores can record regional climatic conditions, highlighting the importance of focusing on the season (DJF) that reflects a clearer signal of local temperature and marine moisture influence.

4 Discussion

4.1 Relationship between the dexc and SIC/SST during the DJF Period

The Hercules Névé record reveals a positive correlation between summer sea-ice concentration (SIC) in the Ross Sea and dexc (Fig. 4A). This association can be understood through the interplay of katabatic winds, sea-ice extent, and polynya processes (Dale et al., 2020; Turner et al., 2016). Under high SIC conditions, katabatic forcing enhances coastal divergence, supporting the persistence of coastal polynyas. These polynyas enhance local evaporation, initially generating vapor with low dexc values due to kinetic fractionation (Merlivat and Jouzel, 1979). Subsequent mixing with continental air masses relatively enriched in dexc (Noone and Simmonds, 2004) modifies the resultant isotopic composition of snowfall. Meanwhile, extensive sea ice coverage modifies the relative contribution of distant, isotopically depleted oceanic sources (Uemura et al., 2008), enhancing the relative influence of locally derived moisture. Comparable mechanisms have been observed in both Antarctic and Arctic regions, where variability in sea-ice extent exerts a strong control on stable isotope compositions (Kurita, 2011; Steen-Larsen et al., 2013).

In contrast, low SIC exposes a broader open-ocean surface, intensifying evaporation under conditions that promote kinetic fractionation and resulting in lower dexc values (Bertler et al., 2018; Kurosaki et al., 2020). This seasonal contrast highlights the role of sea-ice extent and polynya activity in modulating the isotopic characteristics of coastal Antarc-

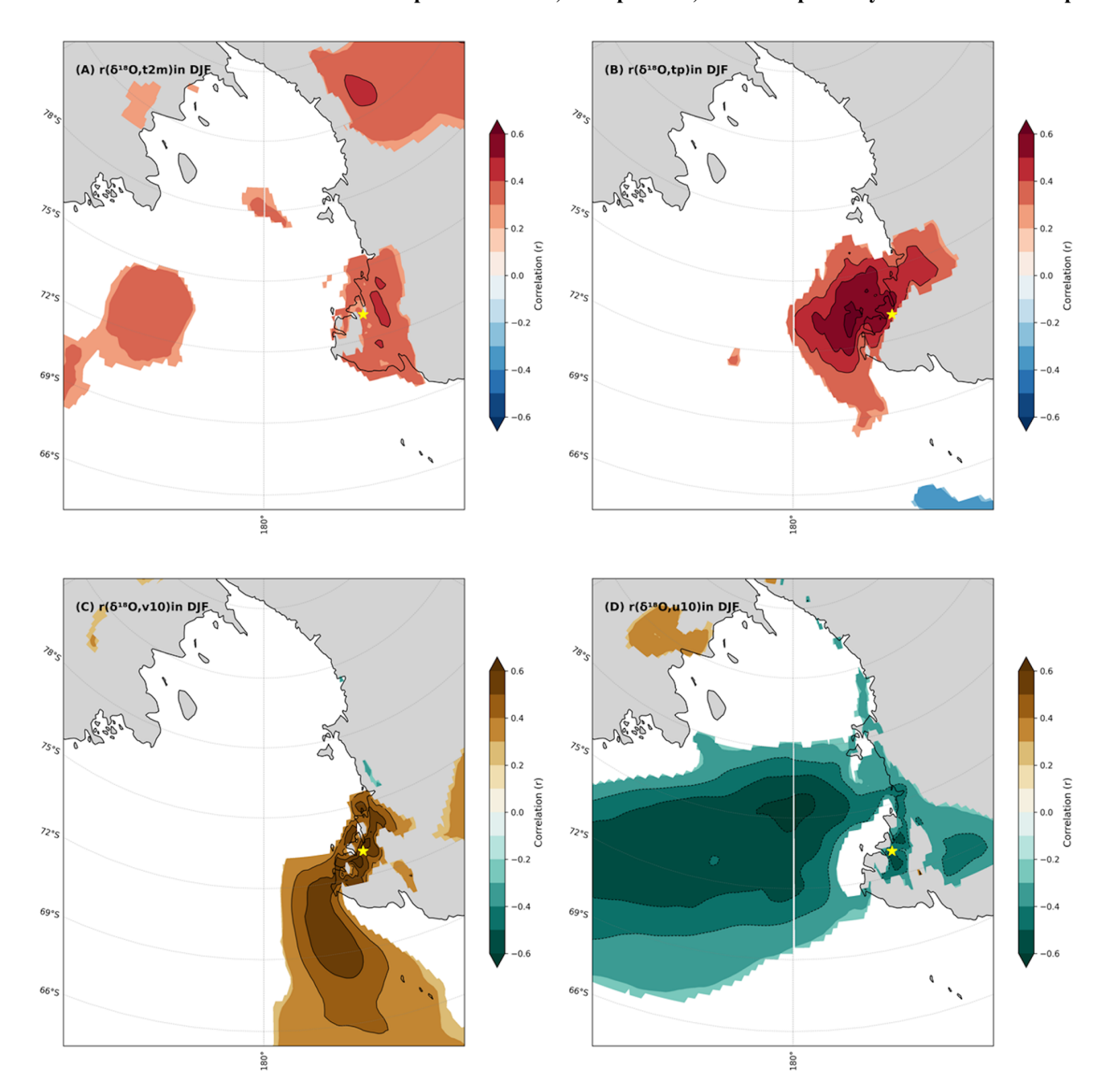


Figure 3. Spatial correlation analysis of (**A**) the 2 m temperature ($T_{2\,\mathrm{m}}$), (**B**) total precipitation (tp), (**C**) 10 m v-wind (v10), and (**D**) 10 m v-wind (u10) across Antarctica based on ERA5 data with δ^{18} O in HN ice core (black symbol) from 1979 to 2015 during DJF. The p < 0.1 confidence level is indicated by black contours.

tic precipitation by altering both moisture source and atmospheric transport pathways. Overall, these findings indicate that isotopic variations in coastal Antarctic precipitation are governed by a combination of sea-ice dynamics, katabatic wind influence, and continental moisture interactions, rather than by temperature alone. This complexity underscores the need to account for source-related processes when interpreting coastal isotope records for paleoclimate applications.

The relationship between dexc and SST further complicates interpretation. Theory anticipates a positive SST–dexc linkage based on fractionation dynamics (Gat et al., 2003; Merlivat and Jouzel, 1979). However, our results reveal a negative correlation between dexc and SST (Fig. 4B), which differs from the expected positive relationship (Merlivat and Jouzel, 1979). We hypothesize that complex ocean–atmosphere interactions in polynya regions, where sea-ice dynamics, variable SST, and atmospheric circulation con-

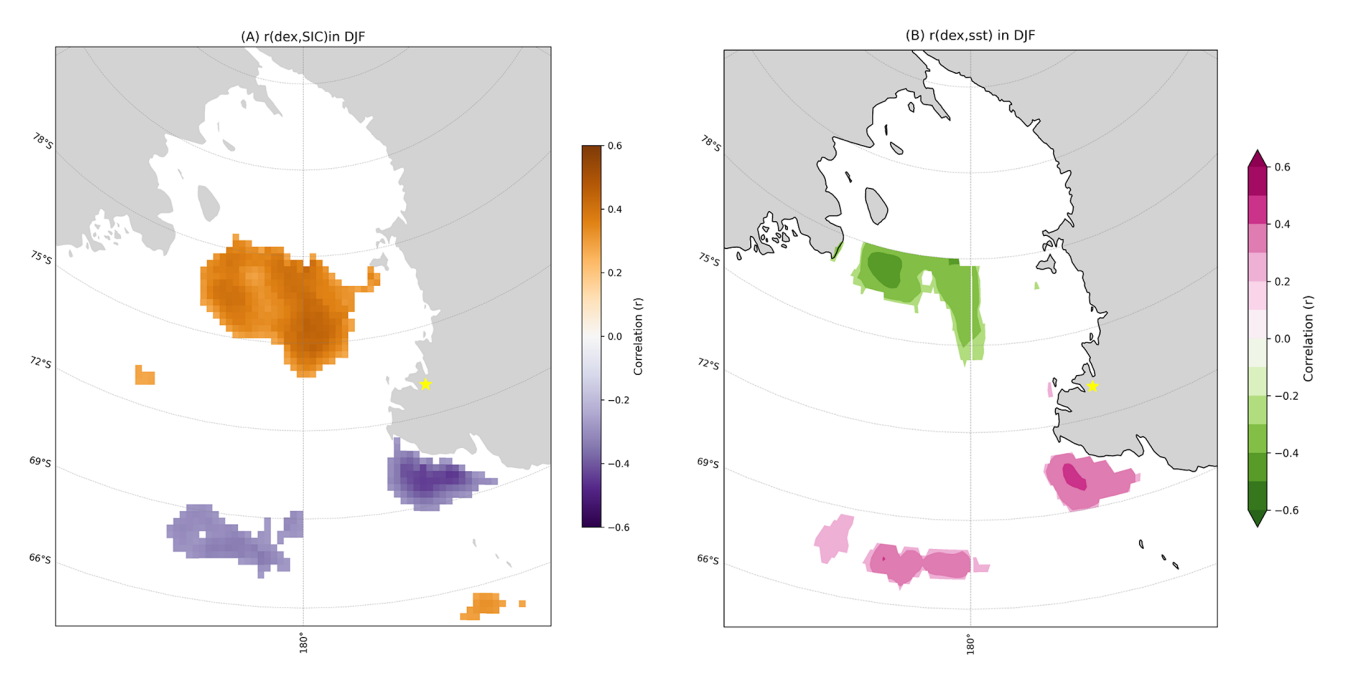


Figure 4. Spatial correlation analysis results between the secondary parameter dexc from the HN ice core (black symbol) and (A) the sea ice concentration (SIC) and (B) sea surface temperature (SST) from ERA5 data during DJF for 1979–2015. The p < 0.1 confidence level is indicated by black contours.

verge, modify the typical SST-d-exc linkage. Further numerical modeling that includes both SST and humidity variability would be necessary to elucidate these processes more precisely (Pfahl and Sodemann, 2014; Uemura et al., 2008). These findings carry two key implications: (1) coastal Antarctic ice core dexc provides a sensitive proxy for sea-ice extent and local air—sea coupling rather than open-ocean temperature, and (2) isotope-based reconstructions using dexc must account for the dominance of polynya processes in regions such as the Ross Sea.

4.2 Influence of the ASL on Water Isotopes and Wind Patterns

The ASL has a profound impact on both δ^{18} O variability and local wind dynamics in the Ross Sea and Victoria Land (Coggins and McDonald, 2015; Turner et al., 2013). In this study, a significant negative correlation was found between ASLrelated mean sea-level pressure and δ^{18} O values in the Hercules Névé region (Fig. 5A). When the ASL intensifies (i.e., its central pressure drops), cold and dry air from the Antarctic continent tends to intrude into the Hercules Névé region, which is associated with more deplete $\delta^{18}O$ in precipitation (Emanuelsson et al., 2023). This observation agrees with prior findings linking a stronger ASL activity to enhanced cold-air advection and lowered isotopic content of snowfall (Hosking et al., 2013; Raphael et al., 2019). Wind patterns also influence the isotopic composition. As discussed in Sect. 3.2, δ^{18} O exhibits a positive correlation with the v-wind (southerly) but a negative correlation with the *u*-wind (westerly), indicating advection of relatively warm, moist versus cold, dry air masses (Fig. 5C–D; Clem et al., 2017).

To further characterize ASL behavior, we conducted a PCA using DJF ASL strength (actual central pressure), latitude, and longitude (Hosking et al., 2013). The first three principal components (PCs) explained all variance in the dataset (PC1: 57.7 %, PC2: 31.2 %, PC3: 11.2 %) (Fig. 6A). PC1 reflects a general displacement toward a stronger, poleward, and eastward ASL but is only weakly associated with δ^{18} O (r = 0.15). PC2 captures a zonal shift with moderate association (r = 0.27), while PC3, though explaining the least variance, exhibits the strongest negative correlation with δ^{18} O (r = -0.34) (Fig. 6B). Loadings (Table 1) indicate that PC3 is characterized by a southward shift in ASL position combined with increased central pressure and slight eastward movement. This coupled ASL pattern appears to be notably associated with changes in the isotopic signature at Hercules Névé, possibly reflecting modified moisture transport pathways. Figure 7 presents the results of the HYS-PLIT back-trajectory clustering for summers with strong and weak ASL conditions, illustrating contrasting transport regimes. During intensified ASL phases in DJF (lower central pressure over the Amundsen Sea), the trajectories indicate that moisture is primarily transported meridionally from the Antarctic interior and the Ross Ice Shelf, producing in longer, more continental air-mass pathways. These conditions correspond to colder, isotopically depleted precipitation with higher dexc values, consistent with enhanced inland and shelf-derived moisture contributions. Conversely, during pe-

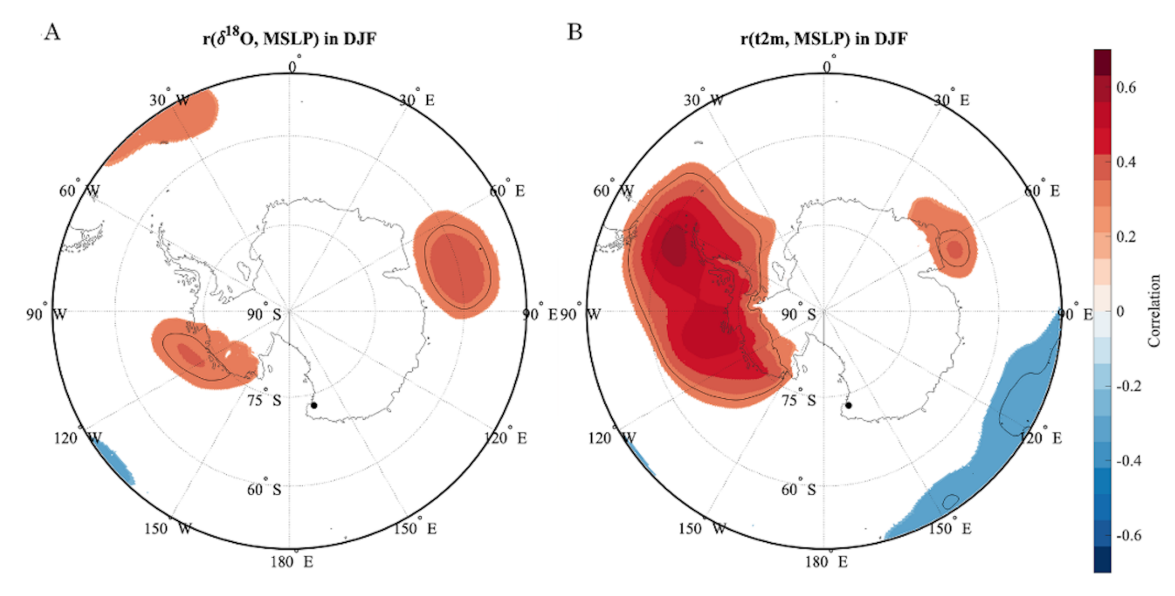


Figure 5. Spatial correlation analysis for (**A**) δ^{18} O from the HN ice core (black symbol) and (**B**) the 2 m temperature ($T_{2\,\text{m}}$) from ERA5 data with the mean sea level pressure (MSLP) from 1979 to 2015 in DJF. Contour plots are used for p < 0.05 and black lines for p < 0.01.

Table 1. PCA loadings of ASL parameters (Actual central pressure, latitude, longitude) from Hosking et al. (2013) datasets. Loadings show variable contributions to each principal component.

Variable	PC1	PC2	PC3
ActCenPres (strength)	0.52	0.69	0.50
Longitude	0.50	-0.73	0.47
Latitude	0.69	0.01	-0.72

riods of a weak ASL phase (higher central pressure), trajectories become more zonal, with increased transport of marine air masses from the open Ross Sea. This pattern is associated with warmer, isotopically enriched precipitation and lower dexc, reflecting the greater influence of oceanic moisture sources. These contrasting circulation regimes demonstrate that ASL variability plays a key role in modulating the origin and isotopic signature of precipitation at Hercules Névé, linking regional-scale atmospheric dynamics to local ice-core records.

In contrast, periods of diminished ASL show an increased proportion of zonal, ocean-originating trajectories, particularly from the Amundsen Sea sector and lower-latitude open waters. These pathways favor the transport of relatively warm, isotopically enriched air and lower dexc values, reflecting a greater contribution of oceanic vapor. This shift underscores the role of large-scale circulation variability in mediating both surface climate and the isotopic imprint preserved in the Hercules Névé ice core. Collectively, these findings indicate that ASL variability is statistically associated with both pressure-related advection and wind-driven changes in regional circulation. Although PC3 explains only

11 % of the total variance, its statistically significant negative correlation with δ^{18} O, emphasizes that structural shifts in ASL circulation importantly influence isotope variability in coastal Antarctica.

4.3 Relationship between ZW3 and Water Isotopes

A significant positive correlation was identified between the DJF seasonal mean strength of ZW3 and δ^{18} O (r = 0.47, p < 0.01) in the Hercules Névé region based on interannual values from 1979 to 2015. The ZW3 index (Goyal et al., 2022) represents monthly variability in the hemispheric wave-3 structure, which we averaged over DJF to align with the period of isotopic signal accumulation in the snowpack. To examine the influence of broader atmospheric circulation patterns, we also examined the Southern Annular Mode (SAM) using principal components from an EOF analysis of 500 hPa geopotential height fields during DJF from ERA5. The first mode (EOF1), associated with SAM, showed no significant relationship with δ^{18} O (r = 0.09, p = 0.58), whereas the second mode (EOF2), consistent with ASL-ZW3 variability, had a statistically significant negative correlation (r = -0.44, p < 0.01). These results suggest that regional wave activity (ZW3) and pressure anomalies (ASL) are more closely associated with δ^{18} O variability in this region than hemispheric SAM variability.

ZW3 is linked to changes in meridional airflow patterns; its intensification enhances the advection of warm, isotopically enriched air masses toward the Ross Sea, resulting in higher δ^{18} O values (Raphael, 2007). While the amplitude of ZW3 strength showed a moderately related to δ^{18} O, the phase of this wave did not exhibit significant influence, indicating that wave amplitude rather than longitudinal displace-

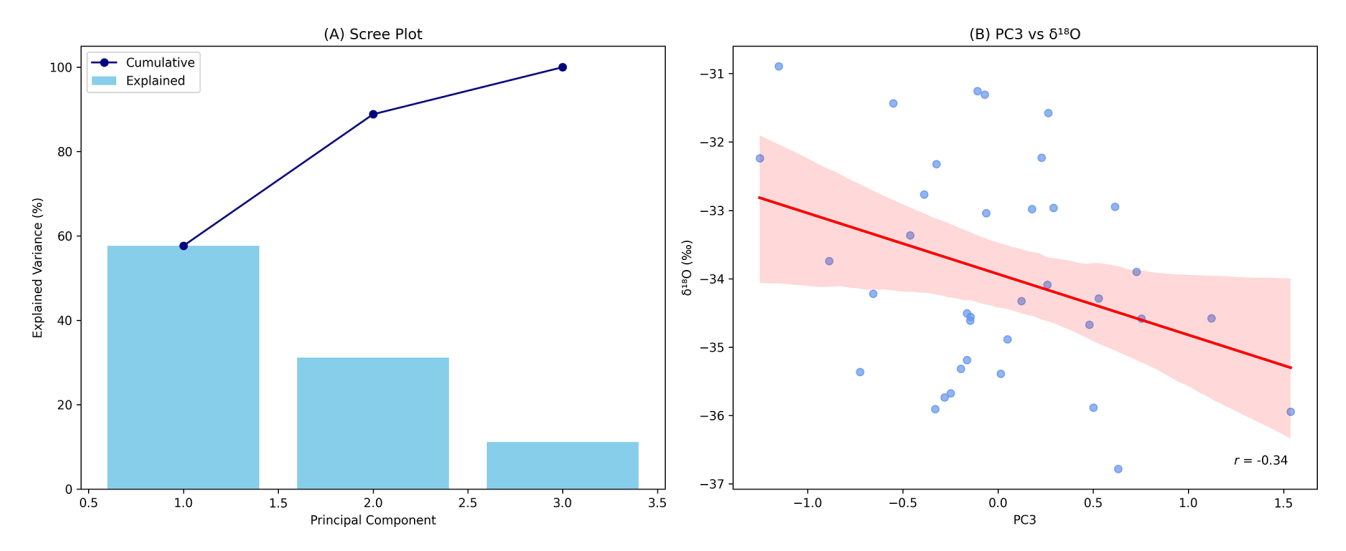


Figure 6. (A) Scree plot showing the variance explained by each principal component derived from ASL monthly variability (central pressure, latitude, and longitude) during DJF (1979–2015). (B) Scatterplot between PC3 and δ^{18} O values from Hercules Névé (r=-0.34), based on DJF-averaged data, showing the strongest correlation among all PCs.

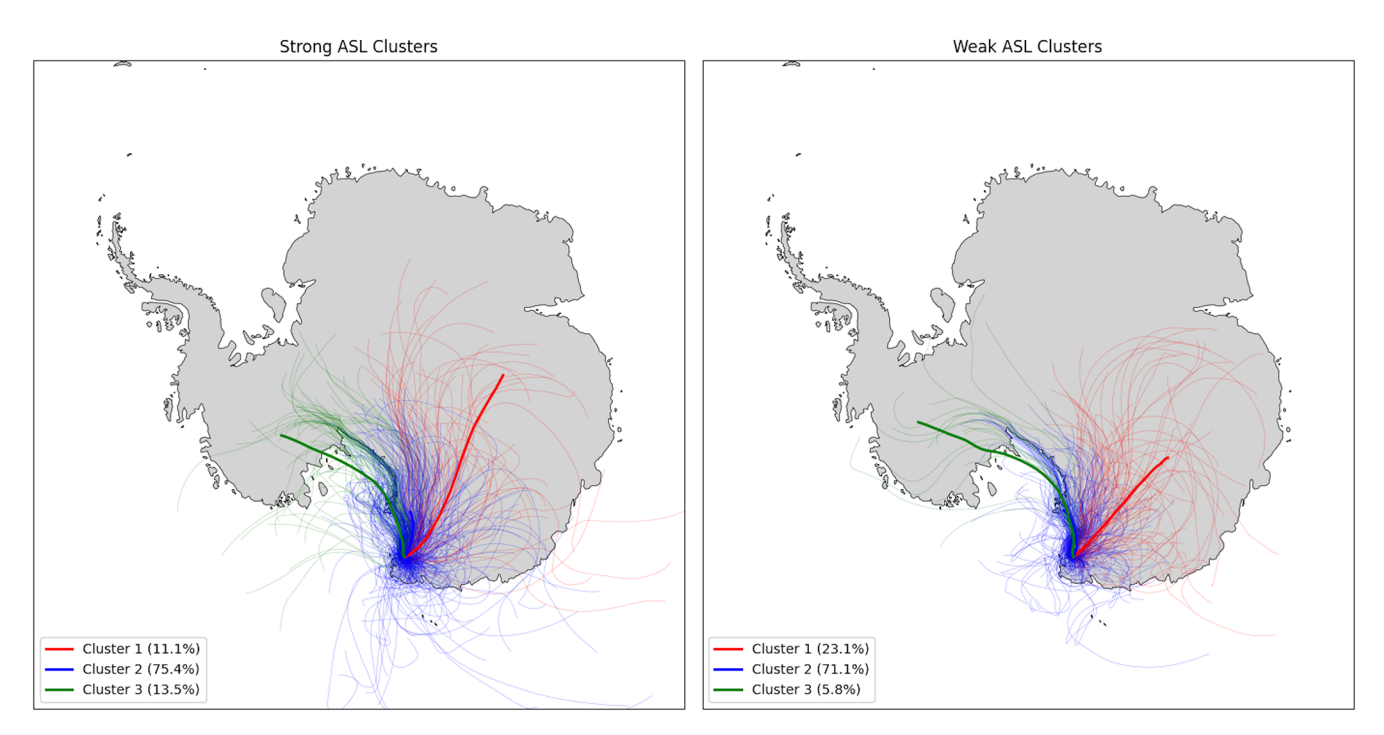


Figure 7. 7 d HYSPLIT back-trajectory clusters arriving at Hercules Névé during (left) the five strongest ASL summers and (right) the five weakest ASL summers (DJF, 1979–2015). Strong ASL cases show dominant air mass transport from inland Antarctica and the Ross Ice Shelf, while weak ASL cases are associated with zonal trajectories originating from the Amundsen Sea and lower-latitude ocean sectors.

ment is more relevant for isotope variability at this site. The interaction between ZW3 and the ASL introduces additional complexity. Enhanced ZW3 activity coincides with increased ASL intensity (Cohen et al., 2013), which can coincide with southward transport of cold, dry continental air, partially offsetting the warming influence of ZW3. This dynamic interplay suggests that δ^{18} O variability at Hercules Névé may rep-

resent a net balance between warm marine and cold continental air mass effects, both associated with the coupled ZW3–ASL system (Hosking et al., 2013; Turner et al., 2013). These findings highlight the importance of considering regional atmospheric wave activity and its coupling with local pressure systems when interpreting isotopic records. Further investigation into the phase relationships and the relative contribu-

tions of competing air masses would be essential to clarify the mechanisms controlling isotope variability in the Ross Sea sector. standing of water-isotope-climate relationships in Antarctica.

5 Conclusions

This study analyzed a Hercules Névé ice core to examine the climatic factors influencing water isotope composition in eastern Antarctica. By investigating the upper 15 m of the 80 m ice core, we identified distinct seasonal variation in the isotopic composition, enabling a high-resolution reconstruction of approximately 40 years of accumulation. This chronology enabled us to trace changes in climate patterns during this period. The analysis focused on the austral summer (DJF), a key period for understanding polynya activity and associated atmospheric processes. Variations in water isotopes, particularly δ^{18} O, are most closely associated with a combination of temperature, precipitation, and wind patterns, with additional associations involving atmospheric pressure systems such as the ASL and ZW3. Southerly winds were associated with enriched δ^{18} O values, while westerly winds were linked to relatively depleted $\delta^{18}O$ values. This pattern highlights the complex relationships between atmospheric dynamics and isotopic composition, where wind direction and intensity may coincide with differences in local climate conditions.

The dexc record from the ice core was positively associated with SIC and negatively associated with SST, which is consistent with katabatic winds and polynya activity along the Ross Sea coast. The intensity of Antarctic winds and the extent of SIC were both linked to precipitation characteristics in the study area, suggesting a connection with local climate variability. The influences of the ASL and ZW3 are also evident in their linkages to isotopic variability. Enhanced ASL activity (lower central pressure) is associated with shifts in wind direction and colder, isotopically depleted precipitation, whereas stronger ZW3 phases correspond to the advection of warm, moisture-rich air and isotopically enriched snowfall. These findings underscore the interconnected nature of regional atmospheric systems and their imprints on Antarctic ice-core records.

Overall, the isotope variability at Hercules Névé reflects the integrated response to temperature, precipitation, wind regimes, and large-scale circulation patterns, rather than temperature alone. This work provides one of the first process-based assessments of summer isotope variability in a coastal Antarctic setting, highlighting how coupled ocean—atmosphere dynamics shape isotopic records. Although the analysis is limited to a single site and season, the results establish a valuable reference framework for interpreting coastal ice-core records. Future studies that incorporate year-round monitoring, extended ice-core datasets, and isotope-enabled atmospheric modeling will further refine our under-

Code availability. No custom or proprietary code was used. All analyses were performed with publicly available open-source software.

Data availability. All water isotope data used in this study are publicly available through the Korea Polar Data Center (KPDC) at https://doi.org/10.22663/KOPRI-KPDC-00001225 (Han and Hur, 2019). No restrictions apply to data access.

Supplement. The supplement related to this article is available online at https://doi.org/10.5194/tc-19-5655-2025-supplement.

Author contributions. This study was conceptualized by YH, SDH and JL. Data were collected by SK, JC, SR and JM. The paper was written by SK, YH and JL, with contributions from all authors.

Competing interests. The contact author has declared that none of the authors has any competing interests.

Disclaimer. Publisher's note: Copernicus Publications remains neutral with regard to jurisdictional claims made in the text, published maps, institutional affiliations, or any other geographical representation in this paper. While Copernicus Publications makes every effort to include appropriate place names, the final responsibility lies with the authors. Views expressed in the text are those of the authors and do not necessarily reflect the views of the publisher.

Acknowledgements. The authors thank colleagues at the Korea Polar Research Institute for logistical support and the reviewers for their constructive comments that improved the manuscript.

Financial support. This research was supported by the Korea Polar Research Institute (grant no. PE25100) and the National Research Foundation of Korea grant funded by the Korean Government (NRF-2022R1A2C3007047). This study was partially supported by the Korea Institute of Marine Science & Technology Promotion (KIMST) and by the Ministry of Oceans and Fisheries (RS-2023-00256677; PM23020).

Review statement. This paper was edited by T. J. Fudge and reviewed by two anonymous referees.

References

- Bertler, N. A. N., Mayewski, P. A., and Carter, L.: Cold conditions in Antarctica during the Little Ice Age Implications for abrupt climate change mechanisms, Earth and Planetary Science Letters, 308, 41–51, https://doi.org/10.1016/j.epsl.2011.05.021, 2011.
- Bertler, N. A. N., Conway, H., Dahl-Jensen, D., Emanuelsson, D. B., Winstrup, M., Vallelonga, P. T., Lee, J. E., Brook, E. J., Severinghaus, J. P., Fudge, T. J., Keller, E. D., Baisden, W. T., Hindmarsh, R. C. A., Neff, P. D., Blunier, T., Edwards, R., Mayewski, P. A., Kipfstuhl, S., Buizert, C., Canessa, S., Dadic, R., Kjær, H. A., Kurbatov, A., Zhang, D., Waddington, E. D., Baccolo, G., Beers, T., Brightley, H. J., Carter, L., Clemens-Sewall, D., Ciobanu, V. G., Delmonte, B., Eling, L., Ellis, A., Ganesh, S., Golledge, N. R., Haines, S., Handley, M., Hawley, R. L., Hogan, C. M., Johnson, K. M., Korotkikh, E., Lowry, D. P., Mandeno, D., McKay, R. M., Menking, J. A., Naish, T. R., Noerling, C., Ollive, A., Orsi, A., Proemse, B. C., Pyne, A. R., Pyne, R. L., Renwick, J., Scherer, R. P., Semper, S., Simonsen, M., Sneed, S. B., Steig, E. J., Tuohy, A., Venugopal, A. U., Valero-Delgado, F., Venkatesh, J., Wang, F., Wang, S., Winski, D. A., Winton, V. H. L., Whiteford, A., Xiao, C., Yang, J., and Zhang, X.: The Ross Sea Dipole – temperature, snow accumulation and sea ice variability in the Ross Sea region, Antarctica, over the past 2700 years, Clim. Past, 14, 193-214, https://doi.org/10.5194/cp-14-193-2018, 2018.
- Casado, M., Landais, A., Picard, G., Münch, T., Laepple, T., Stenni, B., Dreossi, G., Ekaykin, A., Arnaud, L., Genthon, C., Touzeau, A., Masson-Delmotte, V., and Jouzel, J.: Archival processes of the water stable isotope signal in East Antarctic ice cores, The Cryosphere, 12, 1745–1766, https://doi.org/10.5194/tc-12-1745-2018, 2018.
- Casado, M., Landais, A., Picard, G., Arnaud, L., Dreossi, G., Stenni, B., and Prié, F.: Water Isotopic Signature of Surface Snow Metamorphism in Antarctica, Geophysical Research Letters, 48, e2021GL093382, https://doi.org/10.1029/2021GL093382, 2021.
- Clem, K. R., Renwick, J. A., and McGregor, J.: Large-Scale Forcing of the Amundsen Sea Low and Its Influence on Sea Ice and West Antarctic Temperature, Journal of Climate, https://doi.org/10.1175/JCLI-D-16-0891.1, 2017.
- Coggins, J. H. J. and McDonald, A. J.: The influence of the Amundsen Sea Low on the winds in the Ross Sea and surroundings: Insights from a synoptic climatology, J. Geophys. Res.-Atmos., 120, 2167–2189, https://doi.org/10.1002/2014JD022830, 2015.
- Cohen, L., Dean, S., and Renwick, J.: Synoptic Weather Types for the Ross Sea Region, Antarctica, Journal of Climate, 26, 636– 649, https://doi.org/10.1175/JCLI-D-11-00690.1, 2013.
- Craig, H.: Isotopic Variations in Meteoric Waters, Science, 133, 1702–1703, https://doi.org/10.1126/science.133.3465.1702, 1961.
- Dale, E. R., Katurji, M., McDonald, A. J., Voss, P., Rack, W., and Seto, D.: A Comparison of AMPS Forecasts Near the Ross Sea Polynya With Controlled Meteorological Balloon Observations, J. Geophys. Res.-Atmos., 125, e2019JD030591, https://doi.org/10.1029/2019JD030591, 2020.
- Dansgaard, W.: Stable isotopes in precipitation, Tellus, 16, 436–468, https://doi.org/10.1111/j.2153-3490.1964.tb00181.x, 1964.
- Davrinche, C., Orsi, A., Agosta, C., Amory, C., and Kittel, C.: Understanding the drivers of near-surface winds in

- Adélie Land, East Antarctica, The Cryosphere, 18, 2239–2256, https://doi.org/10.5194/tc-18-2239-2024, 2024.
- Emanuelsson, B. D., Renwick, J. A., Bertler, N. A. N., Baisden, W. T., and Thomas, E. R.: The role of large-scale drivers in the Amundsen Sea Low variability and associated changes in water isotopes from the Roosevelt Island ice core, Antarctica, Clim. Dynam., 60, 4145–4155, https://doi.org/10.1007/s00382-022-06568-8, 2023.
- Faber, A.-K., Møllesøe Vinther, B., Sjolte, J., and Anker Pedersen, R.: How does sea ice influence δ^{18} O of Arctic precipitation?, Atmos. Chem. Phys., 17, 5865–5876, https://doi.org/10.5194/acp-17-5865-2017, 2017.
- Fernandoy, F., Meyer, H., Oerter, H., Wilhelms, F., Graf, W., and Schwander, J.: Temporal and spatial variation of stable-isotope ratios and accumulation rates in the hinterland of Neumayer station, East Antarctica, Journal of Glaciology, 56, 673–687, https://doi.org/10.3189/002214310793146296, 2010.
- Frezzotti, M., Urbini, S., Proposito, M., Scarchilli, C., and Gandolfi, S.: Spatial and temporal variability of surface mass balance near Talos Dome, East Antarctica, Journal of Geophysical Research: Earth Surface, 112, https://doi.org/10.1029/2006JF000638, 2007.
- Gat, J. R., Klein, B., Kushnir, Y., Roether, W., Wernli, H., Yam, R., and Shemesh, A.: Isotope composition of air moisture over the Mediterranean Sea: an index of the air-sea interaction pattern, Tellus B, 55, 953–965, https://doi.org/10.1034/j.1600-0889.2003.00081.x, 2003.
- Goursaud, S., Masson-Delmotte, V., Favier, V., Orsi, A., and Werner, M.: Water stable isotope spatio-temporal variability in Antarctica in 1960–2013: observations and simulations from the ECHAM5-wiso atmospheric general circulation model, Clim. Past, 14, 923–946, https://doi.org/10.5194/cp-14-923-2018, 2018.
- Goyal, R., Jucker, M., Gupta, A. S., and England, M. H.: A New Zonal Wave-3 Index for the Southern Hemisphere, Journal of Climate, https://doi.org/10.1175/JCLI-D-21-0927.1, 2022.
- Han, Y. and Hur, S. D.: Isotopic and meteorological data from Hercules Névé, East Antarctica (2016–2019), Korea Polar Data Center (KPDC) [data set], https://doi.org/10.22663/KOPRI-KPDC-00001225, 2019.
- Han, Y., Jun, S. J., Miyahara, M., Lee, H.-G., Ahn, J., Chung, J. W., Hur, S. D., and Hong, S. B.: Shallow icecore drilling on Styx glacier, northern Victoria Land, Antarctica in the 2014–2015 summer, jgsk, 51, 343, https://doi.org/10.14770/jgsk.2015.51.3.343, 2015.
- Helsen, M. M., van de Wal, R. S. W., van den Broeke, M. R., Masson-Delmotte, V., Meijer, H. A. J., Scheele, M. P., and Werner, M.: Modelling the isotopic composition of Antarctic snow using backward trajectories: simulation of snow pit records, Journal of Geophyical Research, 111, D15109, https://doi.org/10.1029/2005JD006524, 2005.
- Hersbach, H., Bell, B., Berrisford, P., Hirahara, S., Horányi, A.,
 Muñoz-Sabater, J., Nicolas, J., Peubey, C., Radu, R., Schepers,
 D., Simmons, A., Soci, C., Abdalla, S., Abellan, X., Balsamo, G.,
 Bechtold, P., Biavati, G., Bidlot, J., Bonavita, M., De Chiara, G.,
 Dahlgren, P., Dee, D., Diamantakis, M., Dragani, R., Flemming,
 J., Forbes, R., Fuentes, M., Geer, A., Haimberger, L., Healy, S.,
 Hogan, R. J., Hólm, E., Janisková, M., Keeley, S., Laloyaux, P.,
 Lopez, P., Lupu, C., Radnoti, G., de Rosnay, P., Rozum, I., Vam-

- borg, F., Villaume, S., and Thépaut, J.-N.: The ERA5 global reanalysis, Quarterly Journal of the Royal Meteorological Society, 146, 1999–2049, https://doi.org/10.1002/qj.3803, 2020.
- Holme, C. T., Gkinis, V., and Vinther, B. M.: Molecular diffusion of stable water isotopes in polar firn as a proxy for past temperatures, Geochimica et Cosmochimica Acta, 225, 128–145, https://doi.org/10.1016/j.gca.2018.01.015, 2018.
- Hosking, J. S., Orr, A., Marshall, G. J., Turner, J., and Phillips, T.: The Influence of the Amundsen–Bellingshausen Seas Low on the Climate of West Antarctica and Its Representation in Coupled Climate Model Simulations, Journal of Climate, https://doi.org/10.1175/JCLI-D-12-00813.1, 2013.
- Hwang, H., Hur, S. D., Lee, J., Han, Y., Hong, S., and Motoyama, H.: Plutonium fallout reconstructed from an Antarctic Plateau snowpack using inductively coupled plasma sector field mass spectrometry, Science of The Total Environment, 669, 505–511, https://doi.org/10.1016/j.scitotenv.2019.03.105, 2019.
- Jackson, S. L., Vance, T. R., Crockart, C., Moy, A., Plummer, C., and Abram, N. J.: Climatology of the Mount Brown South ice core site in East Antarctica: implications for the interpretation of a water isotope record, Clim. Past, 19, 1653–1675, https://doi.org/10.5194/cp-19-1653-2023, 2023.
- Johnsen, S. J., Dahl-Jensen, D., Gundestrup, N., Steffensen, J. P., Clausen, H. B., Miller, H., Masson-Delmotte, V., Sveinbjörnsdottir, A. E., and White, J.: Oxygen isotope and palaeotemperature records from six Greenland ice-core stations: Camp Century, Dye-3, GRIP, GISP2, Renland and NorthGRIP, J. Quaternary Science, 16, 299–307, https://doi.org/10.1002/jqs.622, 2001.
- Jouzel, J., Alley, R. B., Cuffey, K. M., Dansgaard, W., Grootes, P., Hoffmann, G., Johnsen, S. J., Koster, R. D., Peel, D., Shuman, C. A., Stievenard, M., Stuiver, M., and White, J.: Validity of the temperature reconstruction from water isotopes in ice cores, J. Geophys. Res., 102, 26471–26487, https://doi.org/10.1029/97JC01283, 1997.
- Kim, S., Han, C., Moon, J., Han, Y., Hur, S. D., and Lee, J.: An optimal strategy for determining triple oxygen isotope ratios in natural water using a commercial cavity ring-down spectrometer, Geosci. J., 26, 637–647, https://doi.org/10.1007/s12303-022-0009-y, 2022.
- Kurita, N.: Origin of Arctic water vapor during the icegrowth season, Geophysical Research Letters, 38, https://doi.org/10.1029/2010GL046064, 2011.
- Kurosaki, Y., Matoba, S., Iizuka, Y., Niwano, M., Tanikawa, T., Ando, T., Hori, A., Miyamoto, A., Fujita, S., and Aoki, T.: Reconstruction of Sea Ice Concentration in Northern Baffin Bay Using Deuterium Excess in a Coastal Ice Core From the Northwestern Greenland Ice Sheet, Journal of Geophysical Research: Atmospheres, 125, e2019JD031668, https://doi.org/10.1029/2019JD031668, 2020.
- Laepple, T., Münch, T., Hirsch, N., Shaw, F., and Hörhold, M.: Limitations of ice cores in reconstructing temperature seasonality, Nature, 637, E1–E6, https://doi.org/10.1038/s41586-024-08181-7, 2025.
- Maggi, V. and Petit, J.-R.: Atmospheric dust concentration record from the Hercules Névé firn core, northern Victoria Land, Antarctica, A. Glaciology, 27, 355–359, https://doi.org/10.3189/S0260305500017729, 1998.
- Mahalinganathan, K., Thamban, M., Ejaz, T., Srivastava, R., Redkar, B. L., and Laluraj, C. M.: Spatial variability and

- post-depositional diffusion of stable isotopes in high accumulation regions of East Antarctica, Front. Earth Sci., 10, https://doi.org/10.3389/feart.2022.925447, 2022.
- Markle, B. R. and Steig, E. J.: Improving temperature reconstructions from ice-core water-isotope records, Clim. Past, 18, 1321–1368, https://doi.org/10.5194/cp-18-1321-2022, 2022.
- Markle, B. R., Bertler, N. A. N., Sinclair, K. E., and Sneed, S. B.: Synoptic variability in the Ross Sea region, Antarctica, as seen from back-trajectory modeling and ice core analysis, Journal of Geophysical Research: Atmospheres, 117, https://doi.org/10.1029/2011JD016437, 2012.
- Masson-Delmotte, V., Delmotte, M., Morgan, V., Etheridge, D., van Ommen, T., Tartarin, S., and Hoffmann, G.: Recent southern Indian Ocean climate variability inferred from a Law Dome ice core: new insights for the interpretation of coastal Antarctic isotopic records, Climate Dynamics, 21, 153–166, https://doi.org/10.1007/s00382-003-0321-9, 2003.
- Masson-Delmotte, V., Hou, S., Ekaykin, A., Jouzel, J., Aristarain, A., Bernardo, R. T., Bromwich, D., Cattani, O., Delmotte, M., Falourd, S., Frezzotti, M., Gallée, H., Genoni, L., Isaksson, E., Landais, A., Helsen, M. M., Hoffmann, G., Lopez, J., Morgan, V., Motoyama, H., Noone, D., Oerter, H., Petit, J. R., Royer, A., Uemura, R., Schmidt, G. A., Schlosser, E., Simões, J. C., Steig, E. J., Stenni, B., Stievenard, M., Van Den Broeke, M. R., Van De Wal, R. S. W., Van De Berg, W. J., Vimeux, F., and White, J. W. C.: A Review of Antarctic Surface Snow Isotopic Composition: Observations, Atmospheric Circulation, and Isotopic Modeling, Journal of Climate, 21, 3359–3387, https://doi.org/10.1175/2007JCLI2139.1, 2008.
- Merlivat, L. and Jouzel, J.: Global climatic interpretation of the deuterium-oxygen 18 relationship for precipitation, J. Geophys. Res., 84, 5029–5033, https://doi.org/10.1029/JC084iC08p05029, 1979.
- Münch, T., Kipfstuhl, S., Freitag, J., Meyer, H., and Laepple, T.: Regional climate signal vs. local noise: a two-dimensional view of water isotopes in Antarctic firn at Kohnen Station, Dronning Maud Land, Clim. Past, 12, 1565–1581, https://doi.org/10.5194/cp-12-1565-2016, 2016.
- Nardin, R., Amore, A., Becagli, S., Caiazzo, L., Frezzotti, M., Severi, M., Stenni, B., and Traversi, R.: Volcanic Fluxes Over the Last Millennium as Recorded in the Gv7 Ice Core (Northern Victoria Land, Antarctica), Geosciences, 10, 38, https://doi.org/10.3390/geosciences10010038, 2020.
- Noone, D. and Simmonds, I.: Associations between $\delta^{18}\mathrm{O}$ of Water and Climate Parameters in a Simulation of Atmospheric Circulation for 1979–95, Journal Of Climate, 15, https://doi.org/10.1175/1520-0442(2002)015<3150:ABOOWA>2.0.CO;2, 2002.
- Noone, D. and Simmonds, I.: Sea ice control of water isotope transport to Antarctica and implications for ice core interpretation, Journal of Geophysical Research: Atmospheres, 109, https://doi.org/10.1029/2003JD004228, 2004.
- Nyamgerel, Y., Han, Y., Kim, S., Hong, S.-B., Lee, J., and Hur, S. D.: Chronological characteristics for snow accumulation on Styx Glacier in northern Victoria Land, Antarctica, J. Glaciol., 66, 916–926, https://doi.org/10.1017/jog.2020.53, 2020.
- Nyamgerel, Y., Han, Y., Hwang, H., Han, C., Hong, S.-B., Do Hur, S., and Lee, J.: Climate-related variabilities in the Styx-M ice core record from northern Victoria Land, East Antarctica, dur-

- ing 1979–2014, Science of The Total Environment, 935, 173319, https://doi.org/10.1016/j.scitotenv.2024.173319, 2024.
- Pfahl, S. and Sodemann, H.: What controls deuterium excess in global precipitation?, Clim. Past, 10, 771–781, https://doi.org/10.5194/cp-10-771-2014, 2014.
- Raphael, M. N.: The influence of atmospheric zonal wave three on Antarctic sea ice variability, Journal of Geophysical Research: Atmospheres, 112, https://doi.org/10.1029/2006JD007852, 2007.
- Raphael, M. N., Marshall, G. J., Turner, J., Fogt, R. L., Schneider, D., Dixon, D. A., Hosking, J. S., Jones, J. M., and Hobbs, W. R.: The Amundsen Sea Low: Variability, Change, and Impact on Antarctic Climate, Bulletin of the American Meteorological Society, 97, 111–121, https://doi.org/10.1175/BAMS-D-14-00018.1, 2016.
- Raphael, M. N., Holland, M. M., Landrum, L., and Hobbs, W. R.: Links between the Amundsen Sea Low and sea ice in the Ross Sea: seasonal and interannual relationships, Clim. Dynam., 52, 2333–2349, https://doi.org/10.1007/s00382-018-4258-4, 2019.
- Risi, C., Bony, S., Vimeux, F., and Jouzel, J.: Water-stable isotopes in the LMDZ4 general circulation model: Model evaluation for present-day and past climates and applications to climatic interpretations of tropical isotopic records, J. Geophys. Res., 115, 2009JD013255, https://doi.org/10.1029/2009JD013255, 2010.
- Scarchilli, C., Frezzotti, M., and Ruti, P. M.: Snow precipitation at four ice core sites in East Antarctica: provenance, seasonality and blocking factors, Clim. Dynam., 37, 2107–2125, https://doi.org/10.1007/s00382-010-0946-4, 2011.
- Schlosser, E., Stenni, B., Valt, M., Cagnati, A., Powers, J. G., Manning, K. W., Raphael, M., and Duda, M. G.: Precipitation and synoptic regime in two extreme years 2009 and 2010 at Dome C, Antarctica – implications for ice core interpretation, Atmos. Chem. Phys., 16, 4757–4770, https://doi.org/10.5194/acp-16-4757-2016, 2016.
- Servettaz, A. P. M., Orsi, A. J., Curran, M. A. J., Moy, A. D., Landais, A., Agosta, C., Winton, V. H. L., Touzeau, A., Mc-Connell, J. R., Werner, M., and Baroni, M.: Snowfall and Water Stable Isotope Variability in East Antarctica Controlled by Warm Synoptic Events, J. Geophys. Res.-Atmos., 125, e2020JD032863, https://doi.org/10.1029/2020JD032863, 2020.
- Sigl, M., Fudge, T. J., Winstrup, M., Cole-Dai, J., Ferris, D., Mc-Connell, J. R., Taylor, K. C., Welten, K. C., Woodruff, T. E., Adolphi, F., Bisiaux, M., Brook, E. J., Buizert, C., Caffee, M. W., Dunbar, N. W., Edwards, R., Geng, L., Iverson, N., Koffman, B., Layman, L., Maselli, O. J., McGwire, K., Muscheler, R., Nishiizumi, K., Pasteris, D. R., Rhodes, R. H., and Sowers, T. A.: The WAIS Divide deep ice core WD2014 chronology Part 2: Annual-layer counting (0–31 ka BP), Clim. Past, 12, 769–786, https://doi.org/10.5194/cp-12-769-2016, 2016.
- Sime, L., Wolff, E., Oliver, K., and Tindall, J.: Evidence for warmer interglacials in East Antarctic ice cores, Nature, 462, 342–345, https://doi.org/10.1038/nature08564, 2009.
- Sinclair, K. E., Bertler, N. A. N., and Ommen, T. D. van: Twentieth-Century Surface Temperature Trends in the Western Ross Sea, Antarctica: Evidence from a High-Resolution Ice Core, Journal of Climate, https://doi.org/10.1175/JCLI-D-11-00496.1, 2012.
- Sinclair, K. E., Bertler, N. A. N., Trompetter, W. J., and Baisden, W. T.: Seasonality of Airmass Pathways to Coastal Antarctica: Ramifications for Interpreting High-Resolution

- Ice Core Records, Journal of Climate, 26, 2065–2076, https://doi.org/10.1175/JCLI-D-12-00167.1, 2013.
- Song, W., Liu, Z., Lan, H., and Huan, X.: Influence of seasonal sea-ice loss on Arctic precipitation δ18O: a GCM-based analysis of monthly data, Polar Research, 42, https://doi.org/10.33265/polar.v42.9751, 2023.
- Stammerjohn, S. E., Maksym, T., Massom, R. A., Lowry, K. E., Arrigo, K. R., Yuan, X., Raphael, M., Randall-Goodwin, E., Sherrell, R. M., and Yager, P. L.: Seasonal sea ice changes in the Amundsen Sea, Antarctica, over the period of 1979–2014, Elementa: Science of the Anthropocene, 3, 000055, https://doi.org/10.12952/journal.elementa.000055, 2015.
- Steen-Larsen, H. C., Masson-Delmotte, V., Sjolte, J., Johnsen, S. J., Vinther, B. M., Bréon, F.-M., Clausen, H. B., Dahl-Jensen, D., Falourd, S., Fettweis, X., Gallée, H., Jouzel, J., Kageyama, M., Lerche, H., Minster, B., Picard, G., Punge, H. J., Risi, C., Salas, D., Schwander, J., Steffen, K., Sveinbjörnsdóttir, A. E., Svensson, A., and White, J.: Understanding the climatic signal in the water stable isotope records from the NEEM shallow firn/ice cores in northwest Greenland, J. Geophys. Res., 116, D06108, https://doi.org/10.1029/2010JD014311, 2011.
- Steen-Larsen, H. C., Johnsen, S. J., Masson-Delmotte, V., Stenni, B., Risi, C., Sodemann, H., Balslev-Clausen, D., Blunier, T., Dahl-Jensen, D., Ellehøj, M. D., Falourd, S., Grindsted, A., Gkinis, V., Jouzel, J., Popp, T., Sheldon, S., Simonsen, S. B., Sjolte, J., Steffensen, J. P., Sperlich, P., Sveinbjörnsdóttir, A. E., Vinther, B. M., and White, J. W. C.: Continuous monitoring of summer surface water vapor isotopic composition above the Greenland Ice Sheet, Atmos. Chem. Phys., 13, 4815–4828, https://doi.org/10.5194/acp-13-4815-2013, 2013.
- Steig, E. J., Morse, D. L., Waddington, E. D., Stuiver, M., Grootes, P. M., Mayewski, P. A., Twickler, M. S., and Whitlow, S. I.: Wisconsinan and Holocene Climate History from an Ice Core at Taylor Dome, Western Ross Embayment, Antarctica, Geografiska Annaler: Series A, Physical Geography, 82, 213–235, https://doi.org/10.1111/j.0435-3676.2000.00122.x, 2000.
- Stein, A. F., Draxler, R. R., Rolph, G. D., Stunder, B. J. B., Cohen, M. D., and Ngan, F.: NOAA's HYSPLIT Atmospheric Transport and Dispersion Modeling System, Bulletin of the American Meteorological Society, 96, 2059–2077, https://doi.org/10.1175/BAMS-D-14-00110.1, 2015.
- Stenni, B., Caprioli, R., Cimino, L., Cremisini, C., Flora, O., Gragnani, R., Longinelli, A., Maggi, V., and Torcini, S.: 200 years of isotope and chemical records in a firn core from Hercules Névé, northern Victoria Land, Antarctica, Ann. Glaciol., 29, 106–112, https://doi.org/10.3189/172756499781821175, 1999.
- Stenni, B., Serra, F., Frezzotti, M., Maggi, V., Traversi, R., Becagli, S., and Udisti, R.: Snow accumulation rates in northern Victoria Land, Antarctica, by firn-core analysis, Journal of Glaciology, https://doi.org/10.3189/172756500781832774, 2000.
- Stenni, B., Proposito, M., Gragnani, R., Flora, O., Jouzel, J., Falourd, S., and Frezzotti, M.: Eight centuries of volcanic signal and climate change at Talos Dome (East Antarctica), Journal of Geophysical Research: Atmospheres, 107, ACL 3-1–ACL 3-13, https://doi.org/10.1029/2000JD000317, 2002.
- Tetzner, D., Thomas, E., and Allen, C.: A Validation of ERA5 Reanalysis Data in the Southern Antarctic Peninsula – Ellsworth Land Region, and Its Implications for Ice Core Studies, Geo-

- sciences, 9, 289, https://doi.org/10.3390/geosciences9070289, 2019
- Tewari, K., Mishra, S. K., Dewan, A., and Ozawa, H.: Effects of the Antarctic elevation on the atmospheric circulation, Theor. Appl. Climatol., 143, 1487–1499, https://doi.org/10.1007/s00704-020-03456-1, 2021.
- Thomas, E. R., van Wessem, J. M., Roberts, J., Isaksson, E., Schlosser, E., Fudge, T. J., Vallelonga, P., Medley, B., Lenaerts, J., Bertler, N., van den Broeke, M. R., Dixon, D. A., Frezzotti, M., Stenni, B., Curran, M., and Ekaykin, A. A.: Regional Antarctic snow accumulation over the past 1000 years, Clim. Past, 13, 1491–1513, https://doi.org/10.5194/cp-13-1491-2017, 2017.
- Town, M. S., Warren, S. G., Walden, V. P., and Waddington, E. D.: Effect of atmospheric water vapor on modification of stable isotopes in near-surface snow on ice sheets, Journal of Geophysical Research: Atmospheres, 113, https://doi.org/10.1029/2008JD009852, 2008.
- Town, M. S., Steen-Larsen, H. C., Wahl, S., Faber, A.-K., Behrens, M., Jones, T. R., and Sveinbjornsdottir, A.: Post-depositional modification on seasonal-to-interannual timescales alters the deuterium-excess signals in summer snow layers in Greenland, The Cryosphere, 18, 3653–3683, https://doi.org/10.5194/tc-18-3653-2024, 2024.
- Turner, J., Phillips, T., Hosking, J. S., Marshall, G. J., and Orr, A.: The Amundsen Sea low, International Journal of Climatology, 33, 1818–1829, https://doi.org/10.1002/joc.3558, 2013.
- Turner, J., Hosking, J. S., Marshall, G. J., Phillips, T., and Brace-girdle, T. J.: Antarctic sea ice increase consistent with intrinsic variability of the Amundsen Sea Low, Clim. Dynam., 46, 2391–2402, https://doi.org/10.1007/s00382-015-2708-9, 2016.

- Uemura, R., Matsui, Y., Yoshimura, K., Motoyama, H., and Yoshida, N.: Evidence of deuterium excess in water vapor as an indicator of ocean surface conditions, J. Geophys. Res., 113, 2008JD010209, https://doi.org/10.1029/2008JD010209, 2008.
- Vihma, T., Tuovinen, E., and Savijärvi, H.: Interaction of katabatic winds and near-surface temperatures in the Antarctic: Katabatic Winds In The Antarctic, J. Geophys. Res., 116, https://doi.org/10.1029/2010jd014917, 2011.
- Waddington, E. D., Steig, E. J., and Neumann, T. A.: Using characteristic times to assess whether stable isotopes in polar snow can be reversibly deposited, Annals of Glaciology, 35, 118–124, https://doi.org/10.3189/172756402781817004, 2002.
- Yan, Y., Spaulding, N. E., Bender, M. L., Brook, E. J., Higgins, J. A., Kurbatov, A. V., and Mayewski, P. A.: Enhanced moisture delivery into Victoria Land, East Antarctica, during the early Last Interglacial: implications for West Antarctic Ice Sheet stability, Clim. Past, 17, 1841–1855, https://doi.org/10.5194/cp-17-1841-2021, 2021.
- Yang, J., Han, Y., Orsi, A. J., Kim, S., Han, H., Ryu, Y., Jang, Y., Moon, J., Choi, T., Hur, S. D., and Ahn, J.: Surface Temperature in Twentieth Century at the Styx Glacier, Northern Victoria Land, Antarctica, From Borehole Thermometry, Geophysical Research Letters, 45, 9834–9842, https://doi.org/10.1029/2018GL078770, 2018.